

Exploring the magnetic field structure of Ap stars using Stokes I, V, Q and U Zeeman signatures*

G.A. Wade

Astronomy Department, University of Toronto at Mississauga, Mississauga, Ontario, Canada L5L 1C6

Abstract.

This paper describes an ongoing programme aimed at obtaining and modeling high-resolution spectropolarimetric observations of magnetic Ap stars in all 4 Stokes parameters. The ultimate goal of this effort is to produce detailed maps of the surface magnetic fields and chemical abundance distributions of these objects. Herein we review our instrumentation, observations, analysis procedures and preliminary model comparisons. We furthermore discuss new results concerning the impact of anomalous dispersion on spectrum synthesis for magnetic Ap stars, the potential of 4-Stokes timeseries for constraining simple models of the magnetic field geometry and chemical abundance distributions, and the outlook for detailed reconstructions of the surface field and abundance structures.

1. Introduction

Investigators have recently achieved considerable success exploring the magnetic field structure of Ap and Bp stars using Stokes I and V Zeeman spectropolarimetric observations (e.g. Mathys & Hubrig, 1997; Bagnulo & Landolfi, 1999; Landstreet & Mathys, 2000) as well as Stokes Q and U net broadband linear polarisation observations (e.g. Wade et al., 1996; Leroy et al., 1996; Bagnulo et al., 2000). These data have demonstrated the value of observations obtained in multiple Stokes parameters for constraining the topologies of the surface magnetic fields of these stars.

At the same time, the detailed exploitation of these data has been limited by the approximate nature of the observational diagnostics, as well as their often schematic or incomplete theoretical interpretation. For example, all of the commonly employed diagnostics ignore the effects of chemical abundance inhomogeneities.

The goal of this programme is to provide a more physically accurate and theoretically interpretable way to constrain the magnetic field structure and chemical abundance distributions of Ap stars. We accomplish this by taking the observation and modeling back to the place where the Zeeman effect occurs: within individual spectral lines. In this paper we describe the instrumental, observational and numerical solutions we have adopted and developed in order to obtain and model high resolution, high signal-to-noise

ratio measurements of the spectral lines of magnetic Ap stars in all four Stokes parameters.

2. The MuSiCoS spectropolarimeter

The 4 Stokes parameter observations were obtained using the MuSiCoS (MULti-Site Coordinated Spectroscopy) spectropolarimeter mounted on the 2 metre Bernard Lyot telescope at the Pic du Midi observatory.

The spectropolarimeter consists of a table-top echelle spectrograph (Baudrand & Bohm, 1992) fed by a double optical fibre directly from a dedicated Cassegrain-mounted polarisation analysis unit (Donati et al., 1999). In one single exposure, this apparatus allows the acquisition of a stellar spectrum in a given polarisation state (Stokes V , Q or U) throughout the spectral range 450 to 660 nm with a resolving power of about 35000.

In Fig. 1 we show the optical layout of the polarisation analysis unit. In normal operation, starlight enters the analyser at the Cassegrain focus. The beam then may optionally pass through a rotatable $\lambda/4$ retarder (in the case of Stokes V observations) or not (in the case of Stokes Q or U observations). The beam then intersects a Savart-type beamsplitter which separates the stellar light into two beams which are respectively polarised along and perpendicular to the instrumental reference azimuth. The analysed beams are then focally reduced to an aperture of $f/2.5$ for injection into the double 50 μm fibre, which transport the light to the spectrograph. The unit is compact, about 30 cm high by 30 cm wide by 15 cm deep

* Based on observations obtained using the MuSiCoS spectropolarimeter at the Pic du Midi observatory, France.

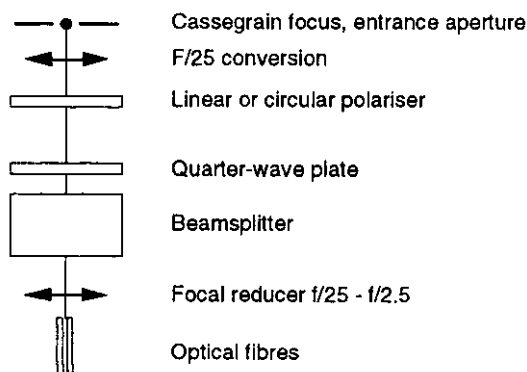


Figure 1: *Optical layout of the MuSiCoS polarisation analysis unit (adapted from Donati et al., 1999).*

(excluding the calibration facilities), and is affixed directly to the TBL Cassegrain bonnet. This arrangement reduced differential mechanical deformation to within about 10 μm , and allows for accurate projection of the orthogonally polarised images onto the fibres.

A complete polarimetric exposure consists of a sequence of 4 subexposures, between which the retarder (for circular polarisation Stokes V) or the instrument itself (for linear polarisations Stokes Q and U) is rotated by $\pm 90^\circ$. This has the effect of exchanging the beams within the whole instrument, and in particular switching the positions of the two orthogonally polarised spectra on the CCD. This observing procedure should in principle suppress all first-order spurious polarisation signatures down to a level of about 0.01% (Donati et al., 1997). The detailed optical characteristics of the polarisation analyser and the spectropolarimetric observing procedures are described by Donati et al. (1999).

3. Observations

We have employed the MuSiCoS spectropolarimeter throughout a total of 50 nights (allocated in 1997 Feb., 1998 Feb., and 1999 Jan.) to obtain both circular and linear polarisation (i.e. 4 Stokes parameter) observations of 12 magnetic Ap stars. For 7 of these stars full rotational phase coverage has been achieved. The full list of stars for which complete Stokes observations were obtained is shown in Table 1.

Circular polarisation Zeeman signatures are detected in essentially all spectral lines of all targets observed, with a typical relative amplitude of $\sim 1\%$. We furthermore detect much weaker linear polarisation Zeeman signatures in the strongest, most magnetically sensitive spectral lines of several of these objects. An example of such a detection is shown

in Fig. 2, for the cool Ap star β Coronae Borealis (Wade et al., 1999a). These represent the first high-quality measurements of stellar spectral line Zeeman linear polarisation ever obtained, and confirm both the general weakness and complexity of Stokes Q and U profiles. A more extensive atlas of the circular and linear polarisation Zeeman signatures in the spectrum of β CrB is provided by Wade (1999).

4. Least-squares deconvolution

While Zeeman linear polarisation is clearly detected in strong, magnetically sensitive spectral lines in many of our highest quality spectra, it is often only marginally detected in strong, sensitive lines in the much more common moderate S/N spectra, and is essentially *never* detected in weaker, less sensitive lines. The lines in which linear polarisation is detected (for example FeII492.393 nm and FeII501.844 nm, both of multiplet 42; Fig. 2) tend to be the strongest and most magnetically sensitive metal lines in the visible spectrum.

In order to increase the absolute S/N of our linear polarisation observations we exploited the information contained in the *many* spectral lines in our echelle spectra. As is discussed by Donati et al. (1997), Least-Squares Deconvolution (or LSD) is a cross-correlation procedure designed for the detection and measurement of such weak polarisation signatures (of order $\sim 0.01 - 1\%$ full amplitude) in stellar spectra. LSD takes advantage of the fact, for weak magnetic fields, that the *shapes* of spectral lines (and associated polarisation features) are approximately the same from one spectral line to another. Donati et al. (1997) develop the procedure for extraction of Stokes V signatures of active late-type stars. Wade et al. (1999a) showed that LSD can also be used for extracting mean linear polarisation Zeeman signatures, and that deconvolution procedures apply which are analogous to that developed by Donati et al. (1997).

In Fig. 3 we illustrate the weak line, weak field homomorphism of which LSD takes advantage. We also show that this homomorphism breaks down in the case of strong fields. This is discussed further in Sect. 6.1.

5. LSD mean Zeeman signatures

LSD was employed to extract mean Zeeman signatures from all Stokes spectra of Ap stars, as well as from numerous Stokes observations of sharp-lined standard stars.

5.1. Standard stars

Cool, sharp-lined nonmagnetic stars were selected as standards in order to diagnose spurious contributions

Table 1: *Magnetic Ap stars with MuSiCoS observations in all 4 Stokes parameters (adapted from Wade et al., 1999a).*

Object	HD number	m_V	Spectral type	Period (days)	# Obs.
Magnetic Ap/Bp stars					
<i>With complete or partial phase coverage</i>					
HD 24712	24712	6.0	A9p SrEuCr	12. ^a 4572	4
HD 32633	32633	7.1	B9p SiCr	6. ^a 43000	13
49 Cam	62140	6.5	A9p SrEu	4. ^a 28679	14
53 Cam	65339	6.0	A2p SrEuCr	8. ^a 02681	10
HD 71866	71866	6.8	A2p EuSr	6. ^a 80022	10
HD 98088	98088	6.2	A3p Sr	5. ^a 905130	3
α^2 CVn	112413	2.9	A0p SiEuHg	5. ^a 46939	18
78 Vir	118022	4.9	A1p SrCrEu	3. ^a 7220	18
β CrB	137909	3.7	A9p SrCrEu	18. ^a 4868	17
<i>With single observations</i>					
HD 81009	81009	6.5	A5pCrSrSi	33. ^a 984	1
Preston's star	126515	7.1	A2p CrSr	129. ^a 95	1
HD 153882	153882	6.3	A1p CrEu	6. ^a 00890	1

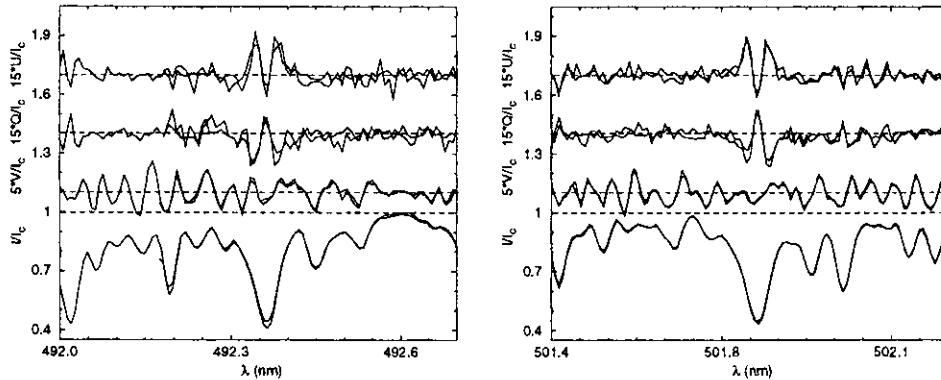


Figure 2: *Stokes I, V, Q and U profiles of β CrB observed for Fe II 492.393 nm and Fe II 501.844 nm on 09 Feb. 1998 (phase 0.64). The agreement of the overlapping échelle orders, along with the reproduction of similar signatures in both lines and LSD profiles, shows clearly that linear polarisation profiles are detected.*

to the line polarisation due to small changes in the position or shape of the observed spectrum either during or between exposures. The 4-subexposure observing procedure we employed (described by Donati et al., 1997) should in principle reduce all spurious signatures in spectral lines down to a level of around 0.01%. In practice, we find (as did Donati et al., 1997)

that episodic signatures several times larger can be produced, although these appear only in our linear polarisation spectra and are thought to be associated with the rotation of the polarimeter module.

Examples of LSD profiles of Arcturus (exhibiting no spurious signatures in Stokes V down to a level of 0.002%, as well as detected spurious signa-

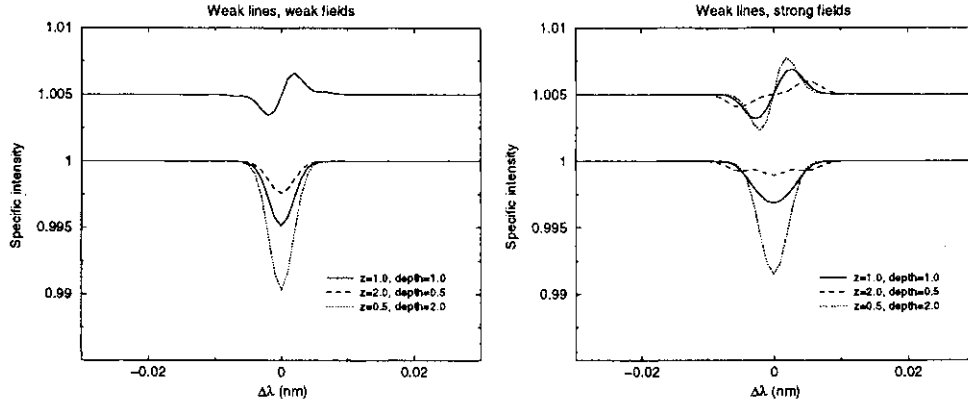


Figure 3: Left frame – Illustrative Stokes I and V profiles for absorption lines of various strengths (characterised by the depth d) and magnetic sensitivities (characterised by the Landé factor z), calculated assuming a weak magnetic field (300 G). All Stokes V profiles have been normalised according to the product $d \cdot z$, and are virtually identical. This homomorphism is the basis of LSD. Right frame – The same profiles for the case of a strong magnetic field (3000 G). Clearly profile homomorphism breaks down in this case. This will be discussed further in Sect. 6.1.

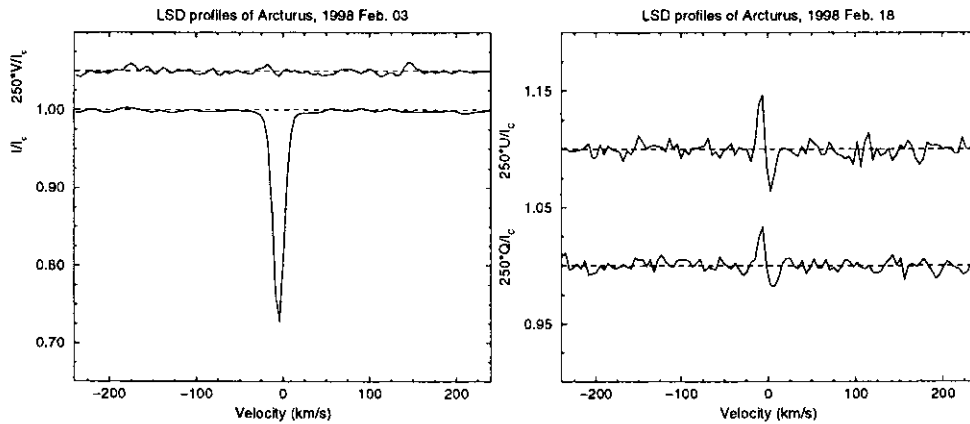


Figure 4: Left – LSD Stokes I and V profiles of the non-magnetic standard star Arcturus. Note that no spurious signatures are detected (down to a relative level of 0.002%). Right – LSD Stokes Q and U signatures of Arcturus. Note the presence of weak (relative full amplitudes of $\sim 0.03\%$) spurious signatures. The Stokes V, Q and U profiles have been expanded and shifted for display purposes.

tures with maximum full amplitude 0.03% in Stokes Q and U) are shown in Fig. 4. Because such spurious signatures scale both with line sharpness and central depth, they are predicted to be much weaker for out typical Ap targets. Wade et al. (1999a) show that potential spurious signatures are negligible for all programme stars.

5.2. Magnetic Ap stars

The magnetic Ap stars for which 4 Stokes parameter observations have been obtained are listed in Table 1. Most of these targets were selected based on successful detection of broadband linear polarisation by Leroy (1995). They are furthermore selected to have relatively low $v \sin i$, and are typically quite bright, both criteria selected in order to improve the poten-

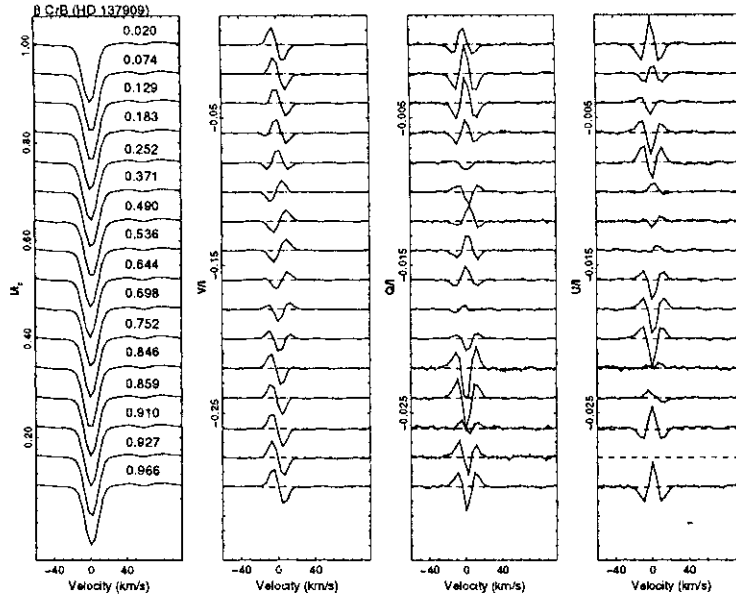


Figure 5: Variation of Stokes I , Q , U and V LSD profiles of β CrB. Rotational phases are shown at left.

tial for detecting the weak linear polarisation signatures. Finally, we have tended to avoid hot stars (in particular He peculiar stars) because of their relatively low line densities and therefore the lower multiplex potential for LSD.

Using LSD, signatures in all four Stokes parameters are consistently detected in the spectral lines of most of our targets. This has allowed us to follow the rotational variation of these profiles for a number of stars.

The LSD profile variations for the slowly-rotating ($v \sin i \lesssim 5 \text{ km s}^{-1}$, $P_{\text{rot}} = 18.49 \text{ d}$), cool FOp star β CrB are shown in Fig. 5. The Stokes Q and U signatures in the spectral lines of this star are especially strong, and are in fact detected in many individual spectral lines at most rotational phases. The linear polarisation signatures of β CrB are the clearest of any star observed in this programme. Correspondingly, the LSD profiles show well-defined, high S/N signatures which are observed to vary clearly throughout the rotational cycle.

In Fig. 6 the LSD Stokes profile variations of the more rapidly rotating ($v \sin i \sim 14 \text{ km s}^{-1}$, $P_{\text{rot}} = 5.47 \text{ d}$) AOp star α^2 CVn are shown. Note the clear Doppler distortion of the mean Stokes I profiles (due to inhomogeneous distributions of the chemical elements, in particular Fe). The variations of Stokes V , Q and U are weaker and more complex than those of β CrB; one can furthermore observe features prop-

agating (due to rotational modulation) through the profiles obtained at successive rotational phases.

The profiles in Figs. 5 and 6 were extracted using full line masks, containing information about spectral lines of all relevant chemical elements. However, LSD can also be used on subsets of such masks which are restricted to single chemical elements. Fig. 7 shows profiles for the A4p star 53 Cam obtained for Fe and Ti submasks. Landstreet (1988) modelled the chemical abundance distributions over the surface of this star, and found Fe to be distributed essentially homogeneously, while Ti showed a very strong surface variation. This is clearly confirmed by these profiles: while the Fe Stokes I profiles show relatively little variation, the Ti profiles vary from near-disappearance to being stronger than the mean Fe profile. The V , Q and U profiles also show significant variability. The morphology of the Fe V , Q and U profiles are substantially different from those of Ti (the difference in the noise level aside; this results from the relatively small number of Ti lines in the spectrum as compared to Fe). This is likely a result of the very different sampling of the magnetic field distribution by these two elements due to their dissimilar surface distributions.

LSD profiles can also be measured to provide more conventional diagnostics of the magnetic field, such as the mean longitudinal magnetic field and net linear polarisation (Donati et al., 1997; Wade et al., 1999b). The measurements are of very high precision, and

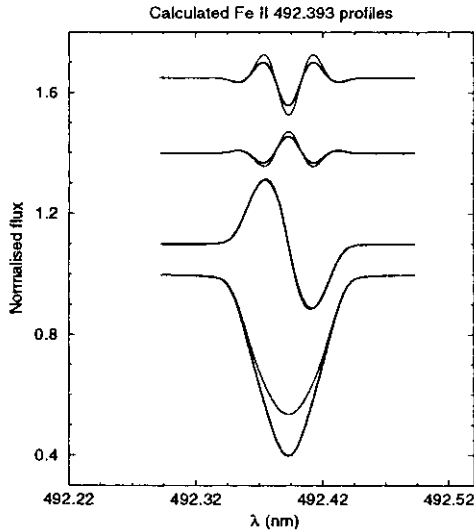


Figure 9: Comparison of Fe II 492.3 nm Stokes I , Q , U and V profiles computed with (heavy lines) and without (fine lines) the effects of anomalous dispersion.

provide a powerful test of the accuracy of the LSD procedure (Wade et al., 1999b). In Fig. 8 we compare measurements of the longitudinal magnetic field of α^2 CVn extracted from LSD Fe profiles, as well as net linear polarisation measurements extracted from LSD profiles of the A2p star 78 Virginis, with previously published observations of these quantities. The agreement between the previously published measurements and those obtained from LSD profiles is excellent. This indicates that LSD produces profiles which have magnetic diagnostic value as good as or better than any other data currently available.

6. Modeling Stokes profiles

Modeling the line profiles of non-magnetic stars requires the solution of the unpolarised transfer problem, which involves a single first-order differential equation. Treatment of the spectral lines of magnetic stars, on the other hand, requires the solution of the polarised transfer problem, involving a set of four coupled first-order differential equations, one for each Stokes parameter.

Landstreet (1988) focused considerable energy developing a code to solve the polarised transfer problem in order to synthesise spectral line profiles of magnetic stars. Because of the cost of computing cycles at the time the code was written, as well as because such effects were thought to have relatively small consequences for Stokes I profiles, magneto-optical effects (or anomalous dispersion) were ignored in the origi-

nal polarised transfer calculation. On the other hand, CPU cycles are now extremely affordable, and furthermore we expected magneto-optical effects to have very important effects on calculated Stokes Q and U profiles. We have therefore substantially modified Landstreet's original line synthesis code to include magneto-optical effects. The resultant code (known as ZEEMAN2) is described in some detail by Wade et al. (2000).

6.1. Impact of magneto-optical effects

To examine the impact on the Stokes profile calculations of including magneto-optical effects, we have performed several comparisons of profiles calculated both with magneto-optical effects turned off, and with magneto-optical effects turned on. Our initial concern was the impact on Stokes Q and U profiles, and magneto-optical effects clearly have important consequences for the inferred linear polarisation amplitude and orientation. However, we were surprised to note that these effects also have, for saturated lines, a very dramatic impact on Stokes I profiles as well. As is shown in Fig. 9, magneto-optical effects can desaturate strong lines, substantially increasing the slope of the curve-of-growth, and resulting in saturated lines which can be much deeper than obtained ignoring magneto-optical effects. Such an effect may well be responsible for the inability of Landstreet et al. (1989) to reproduce the core depths of strong lines of Fe, Ti, Cr and Si in the spectrum of the strongly-magnetic star HD 215441. It probably also affects somewhat the abundance distribution determined by Landstreet (1988) for the Ap star 53 Cam. This is quite important, as Landstreet's model of 53 Cam has been used for a number of important tests of the diffusion theory (e.g. Babel & Michaud, 1991).

This remarkable desaturating effect on Stokes I profiles, as well as the important impact on Stokes Q and U profiles, has been verified using two other independent polarised spectrum synthesis codes (as part of a larger study by Wade et al., 2000). A similar increase in the equivalent width of Stokes I profiles upon the inclusion of magneto-optical effects was noted by Landolfi et al. (1989). These results do not appear to be consistent with the statement by Vasilchenko et al. (1996) that magneto-optical effects have negligible impact on the Stokes profiles of hotter Ap stars.

6.2. Modeling LSD profiles

Because LSD profiles are in fact calculated using the profiles of many individual spectral lines, it is not immediately evident that it should be possible to reproduce their shapes or variations using the parameters of any single spectral line. A simpleminded exami-

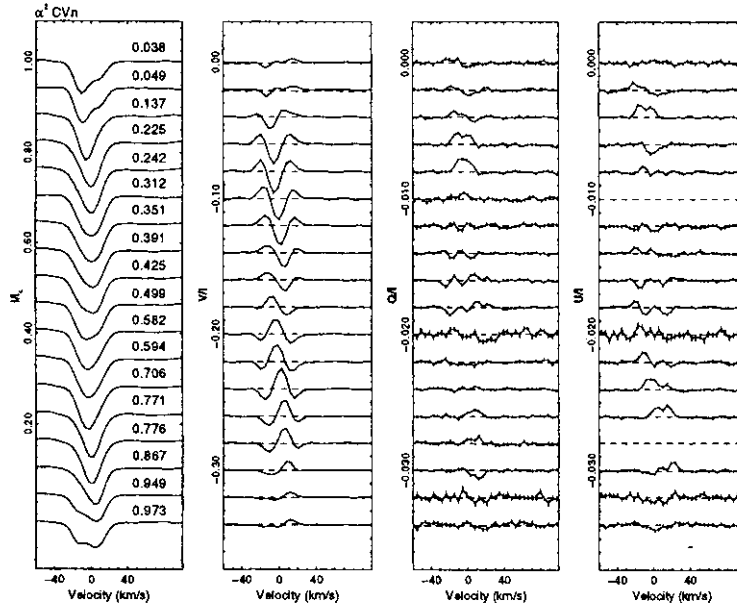


Figure 6: Variation of Stokes I , Q , U and V LSD profiles of α^2 CVn. Rotational phases are shown at left.

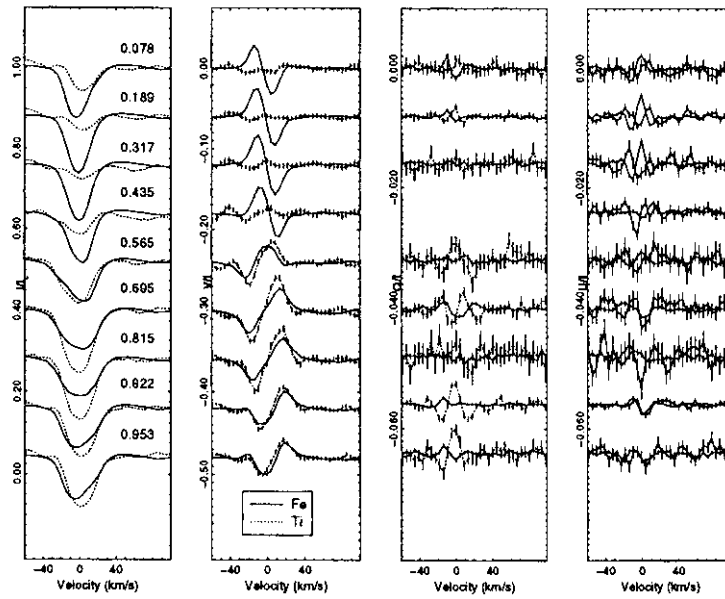


Figure 7: Comparison of Fe and Ti Stokes I , Q , U and V LSD profiles of 53 Cam. Rotational phases are shown at left.

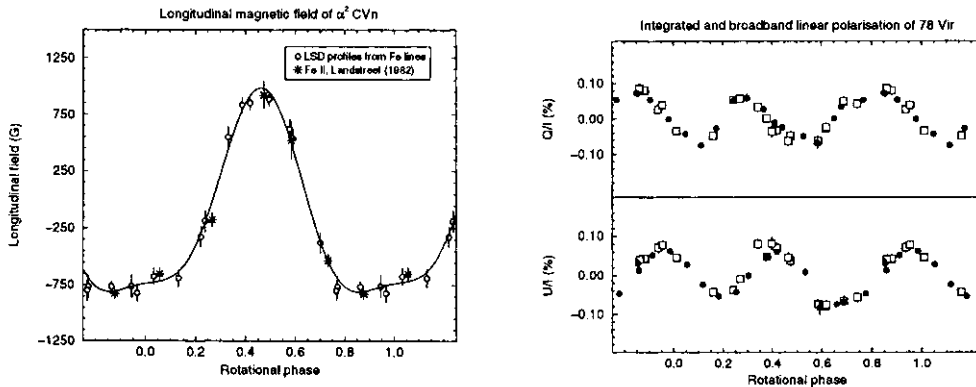


Figure 8: Left frame – comparison of mean longitudinal magnetic field measurements B_l obtained from Fe LSD profiles of α^2 CVn (open circles) and those reported by Landstreet (1982) from observations within a single Fe II line (asterisks). Right frame – comparison of scaled net linear polarisation measurements obtained from LSD profiles of 78 Vir (filled circles) and the broadband linear polarisation measurements by Leroy (1995) (open squares).

nation of Fig. 3 suggests that, even if such an approach may be appropriate in the case of weak fields (where the LSD model seems to be apply), it seems very unlikely to produce reasonable results in the case of strong fields (where the LSD model clearly breaks down).

This is in fact exactly what was shown by Wade (1998) for the special case of a Zeeman triplet. Wade calculated synthetic spectra in the four Stokes parameters for specified magnetic field configurations, and extracted from those spectra LSD profiles which were subsequently fit using a Zeeman triplet line profile model. Spectra were calculated for mean field moduli $\langle H \rangle$ of 0.5, 2, 4, 8 and 12 kG. While the Stokes I and V LSD profiles were reasonably well reproduced by the triplet model for $\langle H \rangle \leq 4$ kG, the Stokes Q and U LSD profiles were observed to exhibit large differences from the triplet model for field moduli as low as 2 kG, and more strikingly the agreement was observed to *degrade* with increasing projected rotational velocity.

A far more sophisticated study of the shapes of LSD profiles, as well as the outlook for reproducing them using relatively simple models, is currently underway (Shorlin, 2001).

While much of this work is still in progress, one conclusion that can be made at this point is that a simple triplet line profile model does not accurately reproduce the LSD profiles of Ap stars with fields stronger than a few kG. As this comprises most of the stars observed by Wade et al. (1999a), modeling of their Stokes profiles (at least initially) must concentrate on the profiles of individual spectral lines.

6.3. Comparison with published models

One application of the new data is to confront the predictions of magnetic field models which have been published previously and which are based on less sophisticated data sets.

Wade et al. (1999a) make such comparisons with models of the Ap stars β CrB, 53 Cam, 49 Cam and HD 71866. In Fig. 10 we reproduce their results for 53 Cam, a comparison of the observed profiles of Fe II 492.393 nm and those prediction assuming the magnetic field/abundance distribution model for this star reported by Landstreet (1988). We first point out the acceptable fit to Stokes I using Landstreet's model without magneto-optical effects (fine curves), and the clearly improved fit when magneto-optical effects are included (heavy curves). This indicates that anomalous dispersion has an important impact on the morphology of Fe II 492.393 nm. Secondly, we note that while the shapes of the Stokes V signatures are approximately reproduced by the model, the amplitude of Stokes V is consistently overestimated. Finally we address the most striking aspect of this comparison: the model substantially overestimates the amplitude of Stokes Q and U at every phase, and at some phases this overestimation is at least 500%. A similar disagreement between the observed and calculated Stokes Q and U profiles has also been encountered by Bagnulo & Wade (in progress) using a non-axisymmetric multipolar model (Bagnulo et al., 1999) determined using various magnetic moments, as well as broadband linear polarisation measurements. This may well provide evidence that the magnetic field of 53 Cam is substantially more complex than has pre-

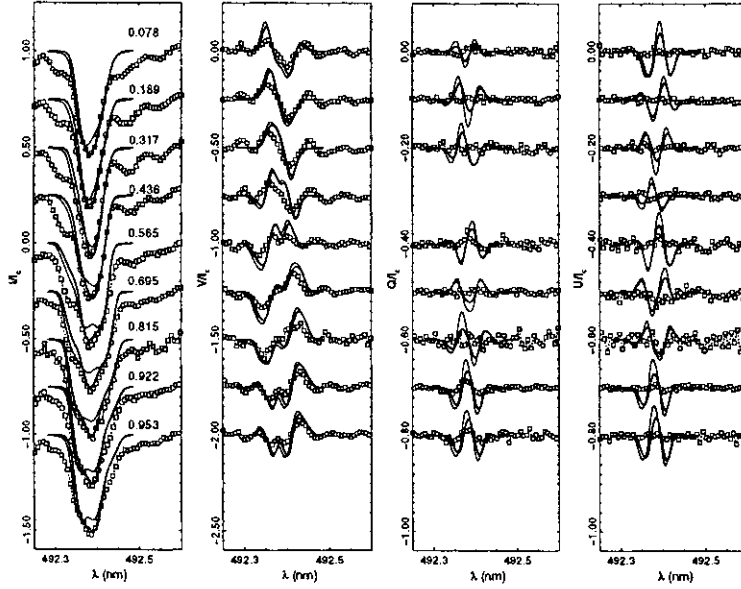


Figure 10: Comparison of observed Fe II 492.3 nm Stokes I, Q, U and V profiles of 53 Cam with the predictions of the model by Landstreet (1988).

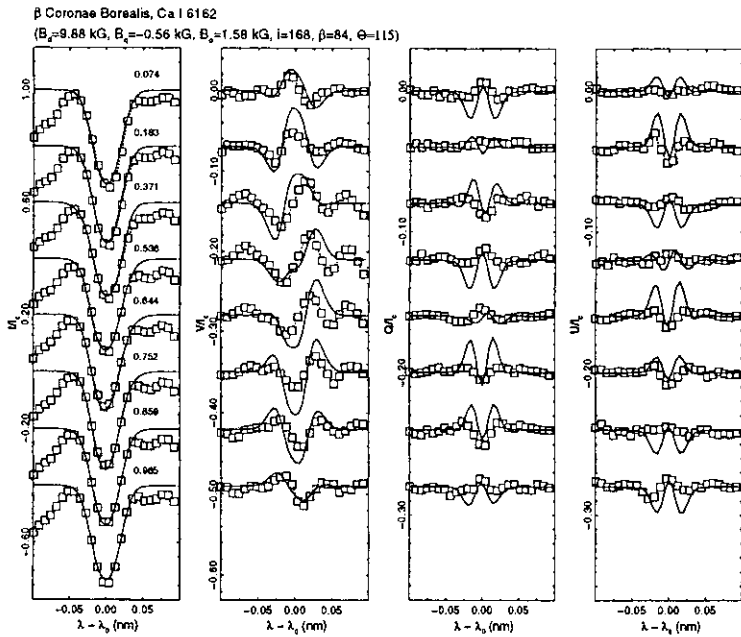


Figure 11: Observed and computed Ca I 616.2 nm Stokes I, V, Q and U profiles of β CrB. The field geometry was obtained by automated least-squares fitting, and corresponds to an oblique rotator with $v \sin i = 3 \text{ km s}^{-1}$, $i = 168^\circ$, $\beta = 84^\circ$ and field moments $B_d = 9.9 \text{ kG}$, $B_q = -0.6 \text{ kG}$ and $B_o = 1.6 \text{ kG}$.

viously been supposed.

6.4. Recovery of the magnetic field configuration

The most exciting potential of the new spectropolarimetric data is their ability to constrain *new* models of the magnetic field configurations, as well as the surface chemical inhomogeneities, of Ap stars. This exploration of this potential is in its early stages.

To date, a few numerical experiments have been conducted to explore the potential of the new data for constraining magnetic and abundance models. For example, the author (Wade, in progress) has examined the ability of the Zeeman signatures to constrain low-order axisymmetric multipolar models of the magnetic field, ignoring and including the effects of abundance nonuniformities. The results of these tests are very encouraging, suggesting that a representative axisymmetric field configuration can be recovered even in the presence of substantial nonaxisymmetric field contributions and/or chemical abundance nonuniformities as large as several dex. In addition, recovery of the axisymmetric configuration can be achieved using high signal-to-noise ratio observations obtained at fewer than 5 rotational phases.

Piskunov (these proceedings) and Kochukov (these proceedings) describe the Magnetic Doppler Imaging technique, essentially the application of the Doppler Imaging procedure to four Stokes parameter observations. This technique is aimed at reconstructing simultaneously both the vector magnetic field distributions and the chemical abundance distribution, without making any *a priori* assumptions about the structure or distribution of either. This technique involves a very large number of free parameters, and therefore requires a substantially larger number of observations in order to obtain a reliable model. On the other hand, the range of possible model configurations is much greater than for a technique such as that described above, and so will no doubt allow for much better reproduction of the observations (although whether or not the resultant models are congruent with reality is always another question!).

In addition to these numerical exercises, a few attempts have been made to actually fit the new data using various models. The author (Wade, in progress) is in the process of employing the axisymmetric modeling procedure described above to reproduce the Stokes profile variations of β Coronae Borealis. In Fig. 11 we show the observed Stokes profile variations of Ca I 616.2 in the spectrum of β CrB, compared with the best-fit axisymmetric magnetic dipole + linear quadrupole + octupole model obtained via least-squares. While the fit to Stokes V , Q and U is clearly only approximate, the model does recover values of the inclination i , the obliquity β , and the mean

field intensity that are comparable to those reported by other authors (e.g. Leroy et al., 1996; Landstreet & Mathys, 2000; Bagnulo et al., 2000). While a nonuniform distribution of Ca was also considered in this modeling, no evidence for line profile variability due to such nonuniformities was found (the resultant uniform Ca abundance was $\epsilon_{Ca} = -5.3$). This is not surprising: the geometry of β CrB results in essentially the same hemisphere of the star being visible throughout an entire rotation. This geometry is illustrated in Fig. 12. Therefore even if surface abundance nonuniformities do exist they will produce little or no line profile variability. Another possibility is that a nonuniform Ca distribution might sample the magnetic equator (say), resulting in Stokes profiles with a different general morphology than would be obtained for a uniform distribution. Again, no evidence for such a scenario was observed.

β CrB is well known to have a non-axisymmetric magnetic field, and so an axisymmetric model such as that described above will only very approximately describe the surface configuration. Bagnulo & Wade (in progress) are studying how the fit to the Stokes profiles can be improved employing a non-axisymmetric multipolar model consisting of a magnetic dipole + general quadrupole. Preliminary fits by least-squares to a few (~ 10) lines simultaneously are encouraging — the agreement between the observed and calculated Stokes profiles is substantially better than that achieved using an axisymmetric model.

7. Outlook

There currently exists a reasonably large collection of four Stokes parameter data suitable for modeling. Based on Table 2 and the figures presented by Wade et al. (1999a), there are 4 stars (53 Cam, β CrB, 78 Vir, α^2 CVn) for which complete Stokes data sets exist for which the observations are of sufficiently quality that modeling of individual spectral lines is possible. There are furthermore three additional objects (49 Cam, HD 32633, HD 71866) for which the observations are probably of insufficient quality for modeling of individual spectral lines, but for which LSD profiles exist. The existence of these observations appears to be motivating a number of investigations aimed at their interpretation, and the full exploitation of these data will likely take a number of years to complete.

Meanwhile, the development of new high-resolution spectropolarimeters (for example the ES-PaDOnS spectropolarimeter for the Canada-France-Hawaii Telescope) continues. This is key, as the brightest, strongest field, sharpest-lined northern Ap stars have already been observed using the MuSiCoS spectropolarimeter, leaving only the more challenging objects, many of which fall outside the capabil-

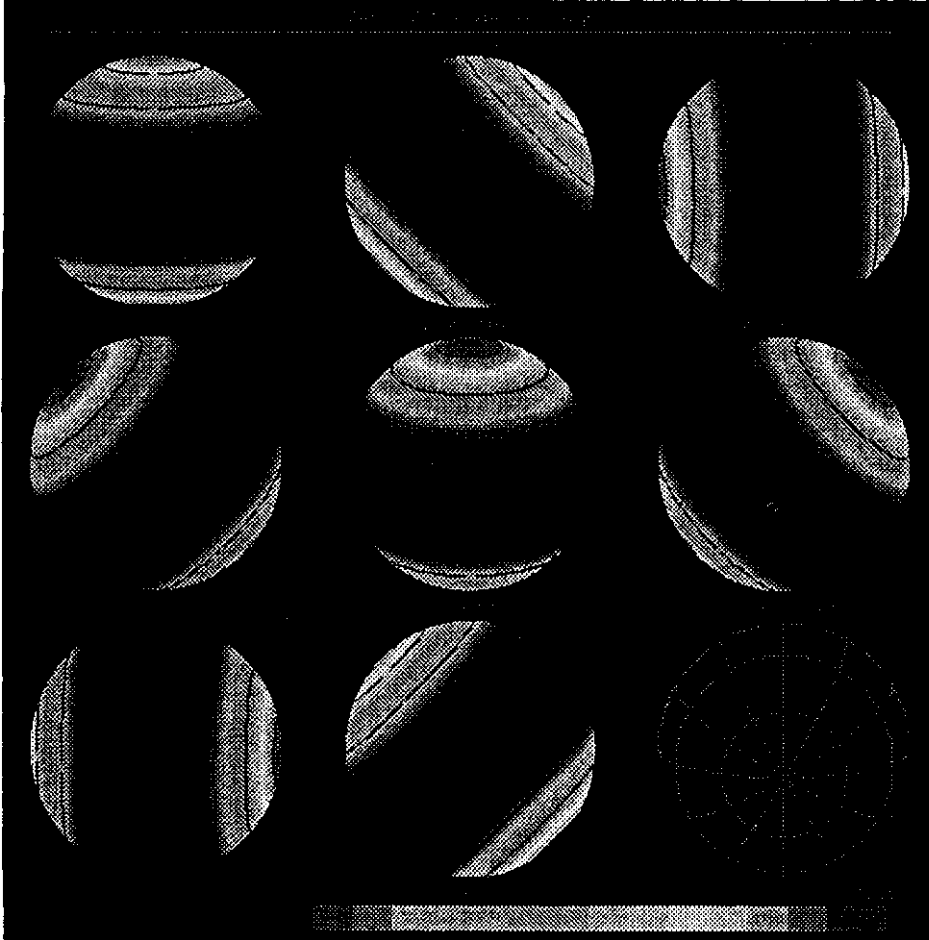


Figure 12: *Surface magnetic field intensity distribution of β CrB corresponding to the axisymmetric model described in the text and in Fig. 11. Individual frames show the field distribution at successive rotational phases, increasing from left to right and top to bottom. The latitude-longitude grid at lower right illustrates the unfavourable geometry of β CrB, viewed nearly at the rotational pole.*

ities of this instrument. New, more sensitive instruments are required to carry on. In addition, while MuSiCoS has the advantage of wide spectral coverage, it can achieve only intermediate ($R = 3.5 \times 10^4$) spectral resolution. Such a resolution corresponds to about 8.5 km s^{-1} , allowing less than 3 resolution elements across the rotationally-broadened line profile of 49 Cam (the most rapidly rotating Ap star for which 4 Stokes parameter results have been obtained to date). Spectropolarimeters with substantially higher resolution ($1 - 2 \times 10^5$) would allow the study of Stokes profiles and the imaging of stellar surfaces with much greater detail.

References

- Babel J., Michaud G., 1991, *Astrophys. J.*, 366, 560
- Bagnulo S., Landolfi M., 1999, *Astron. Astrophys.*, 436, 158
- Bagnulo S., Monin D., Leone F., Stift M.J., 2000, in this book
- Bagnulo S., Mathys G., Landolfi M., Landi Degl'Innocenti M., 2000, *Astron. Astrophys.*, in press
- Baudrand J., Bohm T., 1992, *Astron. Astrophys.*, 259, 711
- Donati J.-F., Catala C., Wade G.A., Gallou G., Delaigue G., Rabou R., 1999, *Astron. Astrophys. Suppl. Ser.*, 134, 149
- Donati J.F., Semel M., Carter B.D., Rees D.E., Cameron A.C., 1997, *Mon. Not. R. Astron. Soc.*, 291, 658
- Landolfi M., Landi Degl'Innocenti M., Landi Degl'Innocenti E., 1989, *Astron. Astrophys.*, 216, 113
- Landstreet J.D., 1982, *Astrophys. J.*, 258, 639

- Landstreet J.D., 1988, *Astrophys. J.*, 326, 967
- Landstreet J.D., Barker P.K., Bohlender D.A., Jewison M.S., 1989, *Astrophys. J.*, 344, 876
- Landstreet J.D., Mathys G., 2000, in preparation
- Leroy J.-L., 1995, *Astron. Astrophys. Suppl. Ser.*, 114, 79
- Leroy J.-L., Landolfi M., Landi Degl'Innocenti E., 1996, *Astron. Astrophys.*, 311, 513
- Mathys G., Hubrig S., 1997, *Astron. Astrophys. Suppl. Ser.*, 124, 475
- Shorlin S.L.S., 2001, Ph.D. Thesis, in preparation
- Vasilchenko D.V., Stepanov V.V., Khokhlova V.L., 1996, *Ast. Letters* 22, 6, 828
- Wade G.A., Elkin V.G., Landstreet J.D., Leroy J.-L., Mathys G., Romanyuk I.I., 1996, *Astron. Astrophys.*, 313, 209
- Wade G.A., 1998, Ph.D. Thesis, The University of Western Ontario, London, Canada, 189
- Wade G.A., 1999, *A Peculiar Newsletter*, 32
- Wade G.A., Donati J.-F., Landstreet J.D., Shorlin S.L.S., 1999a, *Mon. Not. R. Astron. Soc.*, in press
- Wade G.A., Donati J.-F., Landstreet J.D., Shorlin S.L.S., 1999b, *Mon. Not. R. Astron. Soc.*, in press
- Wade G.A., Bagnulo S., Kochukov O., Landstreet J.D., Piskunov N., Stift M.J., 2000, in preparation